

## Chapter 2

# Fine Description of Materials

*[On quantum mechanics] I don't like it, and I'm sorry I ever had anything to do with it.*

—Erwin Schroedinger

Nano-science and nano-technology, as well as fine modeling of the structure and mechanics of materials from nanometric to micrometric scales use descriptions ranging from the quantum to statistical mechanics. Here we revisit modeling at these scales, pointing out the main challenges related to the numerical solution of such models that sometimes are discrete but involve an extremely large number of particles (as it is the case of molecular dynamics simulations or coarse-grained molecular dynamics) and other times are continuous but they are defined in highly multidimensional spaces leading to the well known curse of dimensionality issues. The curse of dimensionality provoked by some of these deterministic models will be emphasized and their numerical implications will be addressed in the second part of this chapter within the PGD framework.

### 2.1 From Quantum Mechanics to Statistical Mechanics: A Walk on the Frontier of the Simulable World

#### 2.1.1 *The Finest Description: The Quantum Approach*

The quantum state of a given electronic distribution could be determined by solving the Schrödinger equation. This equation for many years has been considered as one of the finest descriptions of the world. However, before focusing on the challenges of its numerical solution, we would like to recall that this equation is not relativistic so fails when applied to describe heavy atoms. Moreover, the Pauli's principle

constraint was introduced in the Schrödinger formalism in an “ad hoc” way and constitutes, as we illustrate later, the main difficulty in its solution.

Some simplifying hypotheses are usually introduced, as for example the Born-Oppenheimer approximation that states that the nuclei can be in first approximation assumed as classical point-like particles, that the state of electrons only depends on the nuclei positions and that the electronic ground state corresponds to the one that minimizes the electronic energy for a nuclear configuration. The Schrödinger equation defines a multidimensional problem whose dimension increases linearly with the number of the electrons in the system.

Thus, the knowledge of a quantum system reduces to the determination of the wavefunction  $\Psi(\mathbf{x}_1, \mathbf{x}_2, \dots, \mathbf{x}_N, t; \mathbf{X}_1, \dots, \mathbf{X}_M)$  (that establishes that the electronic wavefunction depends parametrically on the nuclei positions  $\mathbf{X}_i$ ) whose evolution is governed by the Schrödinger equation:

$$i\hbar \frac{\partial \Psi}{\partial t} = -\frac{\hbar^2}{2m_e} \sum_{e=1}^{e=N} \nabla_e^2 \Psi + \sum_{e=1}^{e=N-1} \sum_{e'=e+1}^{e'=N} V_{ee'} \Psi + \sum_{e=1}^{e=N} \sum_{n=1}^{n=M} V_{en} \Psi \quad (2.1)$$

where  $N$  is the number of electrons and  $M$  the number of nuclei, the last ones assumed located and fixed at positions  $\mathbf{X}_j$ . Each electron is defined in the whole physical space  $\mathbf{x}_j \in \mathbb{R}^3$ ,  $i = \sqrt{-1}$ ,  $\hbar$  represents the Planck's constant divided by  $2\pi$  and  $m_e$  is the electron mass.

The differential operator  $\nabla_e^2$  is defined in the conformation space of each electron, i.e.:  $\nabla_e^2 \equiv \frac{\partial^2}{\partial x_e^2} + \frac{\partial^2}{\partial y_e^2} + \frac{\partial^2}{\partial z_e^2}$ . The Coulomb's potentials accounting for the electron-electron and electron-nuclei interactions are written:

$$V_{ee'} = \frac{(q_e)^2}{\|\mathbf{x}_e - \mathbf{x}_{e'}\|} \quad (2.2)$$

$$V_{en} = -\frac{q_n q_e}{\|\mathbf{x}_e - \mathbf{X}_n\|} \quad (2.3)$$

The electron charge is represented by  $q_e$  and the nuclei charge by  $q_n = |q_e| \cdot Z$  (where  $Z$  is the atomic number).

The time independent Schrödinger equation (from which one could determine the ground state, perform quantum static computations or accomplish separated representations of the time-dependent solution) is written:

$$-\frac{\hbar^2}{2m_e} \sum_{e=1}^{e=N} \nabla_e^2 \Psi + \sum_{e=1}^{e=N-1} \sum_{e'=e+1}^{e'=N} V_{ee'} \Psi + \sum_{e=1}^{e=N} \sum_{n=1}^{n=M} V_{en} \Psi = E \Psi \quad (2.4)$$

where the ground state corresponds to the eigenfunction  $\Psi_0$  associated with the most negative eigenvalue  $E_0$ .

Several techniques have been proposed for solving this equation. Some of them lie in the direct solution of the (time-independent or time-dependent) Schrödinger equation. Due to the curse of dimensionality its solution was only possible for very reduced populations of electrons.

Other solution strategies are based on the Hartree-Fock (HF) approach and its derived approaches (post-Hartree-Fock methods). The main assumption of this approach lies in the approximation of the joint electronic wavefunction (related to the  $N$  electrons) as a product of  $N$  3D-functions (the molecular orbitals) verifying the antisymmetry restriction derived from the Pauli's principle. Thus, the original HF approach consists of writing the joint wavefunction from a single Slater's determinant. The Schrödinger equation allows computing the  $N$  molecular orbitals after solving the resulting strongly nonlinear problem. This technique has been extensively used in quantum chemistry to analyze the structure and behavior of molecules involving a moderate number of electrons. Of course, the HF assumption represents sometimes a too crude approximation which invalidates the derived results.

To circumvent this crude approximation different multi-determinant approaches have been proposed. Interested readers can refer to the excellent overview of Cancès et al. [1] as well as the different chapters of the handbook on computational chemistry [2]. The simplest possibility consists in writing the solution as a linear combination of some Slater determinants built by combining  $n$  molecular orbitals, with  $n > N$ . These molecular orbitals are assumed known (e.g. the orbitals related to the hydrogen atom) and the weights are searched to minimize the electronic energy. When the molecular orbitals are built from the Hartree-Fock solution (by employing the ground state and some excited eigenfunctions) the technique is known as the Configuration Interaction method (CI). A more sophisticated technique consists in writing this many-determinants approximation of the solution by using a number of molecular orbitals  $n$  (with  $n > N$ ) assumed unknown. Thus, the minimization of the electronic energy leads to compute simultaneously the molecular orbitals as well as the associated coefficients of this many-determinants expansion. Obviously, each one of these unknown molecular orbitals are expressed in an appropriate functional basis (e.g. gaussian functions, ...). This strategy is known as a Multi-Configuration Self-Consistent Field (MCSCF).

All the just mentioned strategies (and others like the coupled cluster or the Moller-Plesset perturbation methods) belong to the family of the wavefunction based methods. In any case all these methods can be only used to solve quantum systems composed of a moderate number of electrons. As we confirm later the main difficulty is not in the dimensionality of the space, but in the use of the Slater determinants (needed to account for the Pauli's principle) whose complexity scales on the factorial of the number of electrons, i.e. in  $N!$

The second family of approximation methods, widely used in quantum systems composed of hundreds, thousands and even millions of electrons, are based on the density functional theory (DFT). These models, more than looking for an expression of the wavefunction (with the associated multi-dimensional issue) look for the electronic distribution  $\rho(\mathbf{x})$  itself. The main difficulties of this approach are related to the expressions of both the kinetic energy of electrons and the inter-electronic

repulsion energy. The second term is usually modelled from the electrostatic self-interaction energy of a charge distribution  $\rho(\mathbf{x})$ . On the other hand the kinetic energy term is also evaluated in an approximate manner (from the electronic distribution itself in the Thomas-Fermi and related orbital-free DFT models or from a system of  $N$  non-interacting electrons—Kohn-Sham models). Obviously, due to the just referred approximations introduced in the kinetic and inter-electronic interaction energies, a correction term is needed, the so-called exchange-correlation-residual-kinetic energy. However, no exact expression of this correction term exists and so different approximate expressions have been proposed and used. Thus, the validity and accuracy of the computed results will depend on the accuracy of the exchange-correlation term that must be fitted for each system.

The models related to the Thomas-Fermi approximation, less accurate in practice because the too phenomenological expression of the kinetic energy coming from the reference system of an uniform non-interacting electron gas, allows us to consider large multi-electronic systems. In a recent work, Gavini et al. [3] performed multi-million atom simulations by employing the Thomas-Fermi-Weizsacker family of orbital-free kinetic energy functionals. On the other hand, the Kohn-Sham based models are a priori more accurate, but they need the computation of the  $N$  eigenfunctions related to the  $N$  lowest eigenvalues of a non-physical atom composed of  $N$  non-interacting electrons.

Transient solutions are very common in the context of quantum gas dynamics (physics of plasma) but are more infrequent in material science when the structure and properties of molecules or crystals are concerned. For this reason, in what follows, we will focus on the solution of the time-independent Schrödinger equation which leads to the solution of the associated multidimensional eigenproblem, whose eigenfunction related to the most negative eigenvalue constitutes the ground state of the system.

Quantum chemistry calculations performed in the Born-Oppenheimer setting consist either (i) in solving the geometry optimization problem, that is, to compute the equilibrium molecular configuration (nuclei distribution) that minimizes the energy of the system, finding the most stable molecular configuration that determines numerous properties like for instance infrared spectrum or elastic constants; or (ii) in performing an *ab initio* molecular dynamics simulation, that is, to simulate the time evolution of the molecular structure according to the Newton law of classical mechanics. Molecular dynamics simulations allow us to compute various transport properties (thermal conductivity, viscosity, ...) as well as some other non-equilibrium properties.

For more details on the mathematical aspects of these models the interested reader can refer to [4–6] and the references therein.

### 2.1.2 From *ab initio* to Molecular Dynamics

Depending on the choice of the method, on the accuracy required, and on the computer facility available, the *ab initio* methods allow today for the simulations of systems

up to ten, one hundred or some million atoms. In time dependent simulations, they are only convenient for small-time simulations, say not more than a picosecond. However, sometimes larger systems are concerned, and for this purpose one must focus on faster approaches, obviously less accurate. Two possibilities exist: the semi-empirical and the empirical approaches. The semi-empirical approaches speed up the *ab initio* methods by profiting from the information coming from experiments or previous simulations. Empirical methods proceed by considering explicitly only the nuclei, by introducing “empirical” potentials leading to the forces acting on the nuclei. Thus, in the stationary setting only the stable configuration is searched, and for this a geometrical optimization (to compute the nuclei equilibrium distribution) is addressed leading to so-called molecular mechanics. The transient setting results in the classical molecular dynamics but now the computation is sped up by many orders of magnitude with respect to the molecular dynamics where the potentials are computed at the *ab initio* level.

Thus, if we assume a population of  $M$  nuclei (of mass  $m_n$ ) and a two-body potential (many-body potentials are also available), now Newton’s law is written for a generic nuclei  $n$ :

$$m_n \frac{d^2 \mathbf{X}_n}{dt^2} = \sum_{k=1, k \neq n} \mathbf{F}_k^n, \quad \forall n \in [1, \dots, M] \quad (2.5)$$

where  $F_k^n$  denotes the force acting on nucleus  $n$  originated by the presence of nucleus  $k$ . Obviously these forces can be computed from the gradient of the assumed inter-particles potentials.

Accurate algorithms for integrating these equations exist. The symplectic Verlet’s scheme is one of the most used. Molecular dynamics simulations are confronted, despite its conceptual simplicity, with diverse difficulties of different nature:

- The first and most important comes, as previously indicated, from the impossibility of using an “exact” interaction potential derived from quantum mechanics. This situation is particularly delicate when we are dealing with some irregular nuclei distributions such as the ones encountered in the neighborhood of defects in crystals (dislocations, crack tips, etc.), interfaces between different materials or in zones where different kinds of nuclei coexist.
- The second one comes from the units involved in this kind of simulations: the nuclei displacements are in the nanometric scale, the energies are of the order of the electron-volts, the time steps are of the order of  $10^{-15}$  s. Thus, because of the limits in the computers precision, a change of units is required, which can be easily performed.
- In molecular dynamics the behavior of atoms and molecules is described in the framework of classical mechanics. Thus, the particles energy variations are continuous. The applicability of MD depends on the validity of this fundamental hypothesis. When we consider crystals at low temperature the quantum effects (implying discontinuous energy variations) are preponderant, and in consequence the matter properties at these temperatures cannot be determined by MD simulations. The use of MD is restricted to temperatures higher than the Debye’s temperature (for

example the Debye's temperature for the Fe  $\alpha \approx 460$  K). This analysis is in contrast to the vast majority of MD simulations carried out nowadays. In fact, higher is the temperature (kinetic energy) and higher results the velocity of particles, requiring shorter time steps in order to ensure the stability of the integration scheme. For this reason, nowadays most of the MD simulations in solid mechanics are carried out at zero degrees Kelvin or at very low temperatures but, as just pointed out, at these temperatures the validity of the computed MD solutions are polluted by the non-negligible quantum effects.

- The prescription of boundary conditions is another delicate task. If the analysis is restricted to systems with free boundary conditions, then the MD simulation can be carried out without any particular treatment. In the other case we must consider a system large enough to ensure that in the analyzed region the impact of the free surfaces can be neglected. Another possibility lies in the prescription of periodic boundary conditions, where an atom leaving the system for example through the right boundary is re-injected in the domain through the left boundary. Moreover, the particles located in the neighborhood of a boundary are influenced by the ones located in the neighborhood of the opposite boundary. The imposition of other boundary conditions is more delicate from both the numerical and the conceptual points of view. For example, what is the meaning of prescribing a displacement on a boundary? Each situation requires a deep analysis in order to define the best (the most physical) way to prescribe the boundary conditions.
- There are other difficulties related to the transient analysis. We consider a thermal system in equilibrium, i.e. a system in which the velocities follow the Maxwell-Boltzmann distribution. Now, we proceed to heat the system. One possibility lies in increasing suddenly the kinetic energy of each particle. Obviously, even if the resulting velocities define a Maxwell-Boltzmann's distribution, the system remains off equilibrium because the partition between kinetic and potential energies is not the appropriate one. For this reason we must proceed to relax the system that evolves from this initial (non-physical) state to the equilibrium one. Another (more physical) possibility lies in the incorporation of a large enough ambient region around the analyzed system, whose particles are initially in equilibrium at the highest temperature. Now, both regions (the system and the ambient) interact, and the system initiates its heating process that reaches its equilibrium some time later. The final state of both evolutions is the same, but the time required to reach it depends on the technique used to induce the heating. The first transient is purely numerical whereas the second one is more physical allowing the identification of some transport coefficients (for example the thermal conductivity).
- Finally the CPU time continues to be the main limitation of MD simulations. The strongest handicap is related to the necessity of considering at each time step and for each particle the influence of all the others particles. Thus, the integration method seems to scale with the square of the number of particles. Even if some computing time savings can be introduced in the neighbor search, the extremely small time steps and the extremely large number of particles required to describe real scenarios, limit considerably the range of applicability of this kind of simulations, that has been accepted to be nowadays of the order of a cubic micrometer,

even when the systems are considered as very low, and then non-physical, temperatures (close to zero degrees Kelvin). We can notice that, despite the impressive advances in the computational availabilities, the high performance computing and the use of massive parallel computing platforms, the state of the art does not allow the treatment of macroscopic systems encountered in practical applications of physics, chemistry and engineering.

The above mentioned difficulties to perform fully molecular dynamics (MD) simulations motivated the proposal of hybrid techniques that apply MD in the regions where the unknown field varies in a non-uniform way (molecular dynamics model) and a standard finite element approximation in those regions where the unknown field variation can be considered as uniform (continuous model). The main questions concerned by these bridging strategies concern: (i) the kinematics representations in both models; (ii) the transfer conditions on the MD and continuous models interface and (iii) the macroscopic constitutive equation employed in the continuous model.

Different alternatives exist, and the construction of such bridges is nowadays one of the most active topics in computational mechanics. The spurious reflection of the high frequency parts of the waves is one of the main issues. We would like only to mention three “families” of bridging techniques, giving some key references in which the interested reader could find other extremely valuable references: (i) the quasi-continuum method proposed by Tadmor and Ortiz [7]; (ii) the multi-scale method proposed by Wagner and Liu [8] and (iii) the methods based on the “Arlequin” approach [9] like the one proposed by Belytschko in [10].

### 2.1.3 Coarse Grained Modeling: Brownian Dynamics

Sometimes one is interested in analyzing the behavior of a system composed by a series of microscopic entities (particles assumed with a null extension) dispersed into another fluid (the solvent). The kinematics of such particles depends, of course, on their interactions with the solvent particles. A real molecular dynamics simulation is definitively forbidden (the nowadays MD simulation feasibilities rarely exceeds the number of particles contained within a cube of one micron of side).

One possibility to reduce the size of the discrete models lies in considering only the particles of interest. The other particles (the ones that constitute the solvent) are not considered explicitly and only their averaged effects are retained in the modeling.

Thus, the motion equation of a particle whose position is described by  $\mathbf{x}_i$ , is governed by the Langevin equation:

$$m \frac{d^2 \mathbf{x}_i}{dt^2} = \xi \left( \frac{d\mathbf{x}_i}{dt} - \mathbf{v}_f(\mathbf{x}_i) \right) + \mathbf{F}_i^{ext}(t); \quad \forall i, \quad (2.6)$$

where  $m$  denotes the particle mass,  $\mathbf{x}_i$  the position of particle  $i$ ,  $\xi$  the friction coefficient,  $\mathbf{v}_f(\mathbf{x}_i)$  the fluid velocity at position  $\mathbf{x}_i$  and  $\mathbf{F}_i^{ext}(t)$  all the other forces acting

on the particle  $i$  (coming from a external potential or from the solvent particles bombardment). We can notice that even if this model doesn't incorporate explicitly the solvent particles population, their effects are taken into account from the drift term  $\xi \left( \frac{d\mathbf{x}_i}{dt} - \mathbf{v}_f(\mathbf{x}_i) \right)$  as well as by the impact forces.

In the last expression the drift term is quite standard, however the external forces acting on each particle deserve some additional comment. In what follows and without any detriment of generality we assume that there are no other forces than the one coming from the solvent particles bombardment and that the solvent is macroscopically at rest, i.e.,  $\mathbf{v}_f = \mathbf{0}$ . The random nature of the interaction force is modelled from a statistical distribution function that becomes fully defined as soon as its mean value and its standard deviation are fixed. Concerning the mean, one expects a null value if the microscopic dynamics are isotropic. Concerning the standard deviation one must proceed within the statistical mechanics framework. In what follows we summarize the main ideas for the derivation of the standard deviation expression.

Let us define  $B_{\Delta t}$

$$B_{\Delta t} = \int_0^{\Delta t} \frac{F^{ext}(t)}{m} dt = \sum_{k=1}^{k=p} \frac{F^{ext}(t_k)}{m} \delta t, \quad (2.7)$$

where we assume that in  $\Delta t$  the particle is subjected to  $p$  impacts from the solvent particles, with  $p \gg 1$ . These impacts are modeled by a constant force  $F^{ext}(t_k)$  that applies for a time  $\delta t$  ( $\Delta t = p\delta t$ ). By invoking the central limit theorem we conclude that  $B_{\Delta t}$  follows a gaussian distribution  $\mathcal{N}(0, q\Delta t)$  because the number of impacts scales linearly with  $\Delta t$ .

Now, to compute  $q$ , one could integrate the Langevin's equation to obtain the equilibrium velocity distribution  $W$ :

$$W\left(\frac{dx}{dt}, t \rightarrow \infty\right) = \sqrt{\frac{\xi}{m\pi q}} e^{-\frac{\xi \left(\frac{dx}{dt}\right)^2}{mq}} \quad (2.8)$$

that must coincide with the Maxwell-Boltzmann one (canonical ensemble), from which we deduce an expression of  $q$ :

$$q = \frac{2\xi k_b T}{m^2} \quad (2.9)$$

where  $k_b$  is the Boltzmann constant and  $T$  the absolute temperature.

Thus, the Langevin equation is fully defined, by writing:

$$B_{\Delta t} = \int_0^{\Delta t} \frac{F^{ext}(t)}{m} dt = \mathcal{N}\left(0, 2\frac{\xi k_b T}{m^2} \Delta t\right) \quad (2.10)$$



an expression that applies also in the presence of other forces like the ones coming from a gradient of a potential or when  $\mathbf{v}_f \neq \mathbf{0}$ .

Thus, one could track the movement of each particle  $\mathbf{x}_i$  by considering a standard drift term and a random force whose distribution is perfectly known. This stochastic approach has been traditionally also used for solving deterministic models as the advection-diffusion one, because one could compute some moments of the resulting distribution by tracking a moderate population of particles instead of discretizing the deterministic counterpart of the advection-diffusion model by using one of the standard mesh-based discretization techniques that could involve in the case of 3D models an excessive number of degrees of freedom.

To illustrate this procedure we consider the simplest form of the advection-diffusion equation:

$$\frac{\partial C}{\partial t} + \mathbf{v} \cdot \nabla C = D \Delta C \quad (2.11)$$

where  $C = C(\mathbf{x}, t)$  is the concentration field and  $D$  is the so-called diffusion coefficient.

Obviously, this simple parabolic equation could be solved by using any standard technique (finite differences, finite elements, spectral methods, finite volumes, the method of particles, ...), but in what follows we are solving it using a stochastic approach. For this purpose we assume the initial condition represented by  $N$ -Dirac masses:

$$C(\mathbf{x}, t = 0) \approx C^0(\mathbf{x}) = \sum_{i=1}^{i=N} c_i \delta(\mathbf{x} - \mathbf{x}_i(t = 0)) \quad (2.12)$$

Here, we are not discussing the choice of the coefficients  $c_i$  and the locations  $\mathbf{x}_i$ . Several possibilities exist to perform a choice trying to represent, as precisely as possible, the initial concentration distribution. Most of them proceed by regularizing the Dirac distribution and then enforcing the minimization of  $\|C(\mathbf{x}, t = 0) - C^0(\mathbf{x})\|$ . From now on,  $c_i$  and  $\mathbf{x}_i(t = 0)$  are assumed known. Moreover, as the considered advection-diffusion equation does not contain source terms, the weights  $c_i$  remain unchanged during the evolution of the pseudo-particles positions  $\mathbf{x}_i(t)$ .

Now, the simplest explicit integration algorithm proceeds by updating the particle position considering both the deterministic and the random contributions:

$$\mathbf{x}_i^{n+1} = \mathbf{x}_i^n + \mathbf{v}(\mathbf{x}_i^n) \Delta t + \mathcal{N}(0, 2D\Delta t)\mathbf{u}, \quad \forall i \quad (2.13)$$

where  $\mathbf{x}_i^{n+1} \equiv \mathbf{x}_i(t = (n + 1) \cdot \Delta t)$  and  $\mathbf{u}$  is a unit random vector.

Now the distribution moments can be easily computed, and the concentration field could be reconstructed by employing some appropriate smoothing.

It is usual to find this kind of advection-diffusion equations in many branches of science and engineering. In particular they are encountered when one models macro-molecular materials within the statistical mechanics framework, as we describe later. Despite its intrinsic simplicity, sometimes they arise defined in high dimensional

spaces including the physical and the conformation coordinates. To avoid the curse of dimensionality drawback characteristic of mesh-based techniques, different authors proposed the use of stochastic techniques exploiting the equivalence between the so-called Fokker-Planck equation and the Ito's stochastic equation [11], similar to the just described equivalence between models (2.11) and (2.13). Thus, if one is only interested in computing some moments of the resulting distribution function a moderate population of particles is enough to describe accurately the evolution of such moments. The size of the pseudo-particles population that must be considered for computing accurately the different moments of the solution scales linearly with the dimension of the space, however, if one wants to reconstruct the distribution itself, an impressive number of particles is required which do not scale anymore linearly with the dimension of the space.

In general the technique just presented, is conceptually very simple and then easy to implement in a computer or in a parallel computing platform. Explicit integration schemes are usually employed, needing for a careful choice and control of the time step.

It is nowadays widely recognized that the main drawbacks of stochastic techniques are: (i) the control of the statistical noise that makes difficult the use of the stochastic approach to perform inverse parameter identification or optimization, because the poor accuracy in the sensitivity analysis; (ii) the difficulty to reconstruct the model solution itself even in moderate multidimensional models; and (iii) the necessity to solve always the transient model, even if one is only interested in the steady state.

Moreover, in complex flows simulation using for example a finite element solver for the flow kinematics computation, one must ensure that all the elements contains a number of particles, at least enough to allow computing the virial stress (the usual micro-macro bridge). Different possibilities exist, but all of them have a non-negligible impact on the solution. Thus, if new particles are added (and probably others removed) the size of the model is changing, tracking procedures are time consuming, and the initialization of the just introduced particles induces a noticeable numerical diffusion.

One could think that the aforementioned difficulties could be circumvented by employing a Lagrangian description of the flow combined with a Lagrangian description of the microstructure evolution (stochastic approach), however usual mesh-based strategies fail because the high distortion of the meshes during the flow. A first tentative strategy of coupling a meshless Lagrangian description of the flow kinematics (using the natural element method widely described in [12, 13]) and a Lagrangian microstructure description have been recently performed in [14]. This technique could be extended for coupling a Lagrangian flow description with a stochastic description of the microstructure evolution. In any case the difficulties just mentioned will persist.

To reduce the computational cost of numerical simulations different model reduction techniques have been recently proposed [15]. However, the coupling of such techniques (based on the proper orthogonal decomposition—also known as Karhunen-Loève decomposition) with a Lagrangian description of the microstructure evolution remains nowadays an open problem. However, sometimes the stochastic model can

be written in an Eulerian form (Brownian Configuration Fields) and in that case, as illustrated in [16], the model reduction runs opening some interesting perspectives.

### 2.1.4 Coming Back to Continuous Descriptions: Kinetic Theory Models

The next level of description concerns statistical mechanics where the knowledge of individuals is substituted by a kind of averaged knowledge described by a probability distribution function that depends on some conformational coordinates depending on the considered model. In what follows we address some models involving more or less large conformational spaces.

#### 2.1.4.1 The Vlasov-Poisson-Boltzmann Equation

Firstly, we consider the dynamics of  $N$  electrically charged particles of mass  $m$ . When  $N$  becomes too large, direct molecular dynamics simulations result to be prohibitive from the computing time viewpoint. Thus, more than describing the system from the position and velocities of all the particles, one could introduce the function  $f(t, \mathbf{x}, \mathbf{v})$  given the number of particles that, at time  $t$ , are located within an elementary volume  $d\mathbf{x} = (dx, dy, dz)^T$  placed at position  $\mathbf{x}$  and having velocities within the volume defined by  $d\mathbf{v} = (du, dv, dw)^T$  around  $\mathbf{v}$ . Now, the density balance is written:

$$\frac{\partial f}{\partial t} + \mathbf{v} \cdot \nabla_{\mathbf{x}} f + \mathbf{a}(\mathbf{x}, t) \cdot \nabla_{\mathbf{v}} f = S(t, \mathbf{x}, \mathbf{v}), \quad (2.14)$$

where  $\nabla_{\mathbf{x}}$  and  $\nabla_{\mathbf{v}}$  represent the gradient operator in the physical and velocity spaces respectively. We assume that the acceleration  $\mathbf{a} = \frac{d\mathbf{v}}{dt}$  does not depend on the velocity (for this reason it is not affected by the velocity-gradient  $\nabla_{\mathbf{v}}$ ). The source term  $S(t, \mathbf{x}, \mathbf{v})$  represents the so-called collision term and can be derived from an appropriate physical analysis.

We do not need any physics to model the velocity field  $\mathbf{v}$  because now the velocity field is a real coordinate, like the spatial ones. On the contrary, we need to define the acceleration field  $\mathbf{a}(\mathbf{x}, t)$ . For this purpose we consider the Newton's law  $\mathbf{a} = \frac{\mathbf{F}}{m}$ , and compute the force acting on the particles by taking into account the nature of the system, that in the case here addressed consists of a population of charged particles interacting by means of the Coulomb's potential. The electrostatic potential  $U(\mathbf{x}, t)$  can be computed by solving the associated Poisson's problem:

$$\Delta U(\mathbf{x}, t) = -4\pi k Q(\mathbf{x}, t), \quad (2.15)$$

where  $k$  is the Coulomb law constant and  $Q(\mathbf{x}, t)$  is the electrical charge inside the volume  $d\mathbf{x}$  around  $\mathbf{x}$  that can be computed from:

$$Q(\mathbf{x}, t) = q \int_{\mathbb{R}^3} f(\mathbf{x}, \mathbf{v}, t) d\mathbf{v}, \quad (2.16)$$

with  $q$  the particle charge. The force acting on a particle can be finally computed by using:

$$\mathbf{F}(\mathbf{x}, t) = -q \nabla_x U(\mathbf{x}, t) \quad (2.17)$$

*Remark 2.1.1*

1. When the particles are not charged the steady state solution of Eq. (2.14) leads to the Maxwell-Boltzmann distribution when the appropriate choice of the collision term representing the particles collisions is made.
2. When the interaction potential does not comply the Coulomb's law, model (2.15)–(2.17) cannot be employed. In this case we must compute the force by using:

$$\mathbf{F}(\mathbf{x}, t) = \int_{\mathbb{R}^3} \mathbf{F}(\mathbf{x}, t; \mathbf{x}') \tilde{f}(\mathbf{x}', t) d\mathbf{x}' \quad (2.18)$$

where

$$\tilde{f}(\mathbf{x}, t) = \int_{\mathbb{R}^3} f(\mathbf{x}, \mathbf{v}, t) d\mathbf{v} \quad (2.19)$$

and  $\mathbf{F}(\mathbf{x}, t; \mathbf{x}')$  represents the force at position  $\mathbf{x}$  originated by a particle located at position  $\mathbf{x}'$ . In any case this analysis fails when (i) the inter-particle potential leads to a non-definite integral (2.18); and (ii) in the case of dense systems where the movements of particles is correlated.

3. When the acceleration does not depend on the velocity (as was assumed in Eq. (2.14)) and the collision terms vanishes, an equivalence between the conservation equation and the Liouville's theorem in the phase space can be established.
4. In general the establishment of collision terms is quite difficult. To circumvent this difficulty and assuming that the equilibrium distribution is known  $f_{eq}(\mathbf{x}, \mathbf{v}, t)$ , one could approximate the collision term by

$$S(t, \mathbf{x}, \mathbf{v}) = \frac{f_{eq}(\mathbf{x}, \mathbf{v}, t) - f(\mathbf{x}, \mathbf{v}, t)}{\tau} \quad (2.20)$$

where  $\tau$  represents a relaxation time. This approximation leads to the so-called BFK models.

5. Equation (2.14), also known as the Vlasov-Poisson-Boltzmann equation, is widely used to model quantum plasmas. One could imagine the extension of this formalism (within the BBGKY hierarchy) to a variety of physical models: colloids, ferrofluids, coarse grained molecular dynamics, crystallization, demixing, etc. The associated kinetic theory descriptions constitute the Vlasov-Fokker-Planck models.

6. The kinetic theory formalism allows transforming a discrete model into its continuous counterpart. However, in general, the continuous descriptions involve highly multidimensional spaces and their evolutions are governed by hyperbolic non-linear partial differential equations. To solve these kind of models appropriate stabilized solvers, able to proceed in highly multidimensional spaces, are needed.

In the previous paragraphs we introduced some ideas related to kinetic theory models of systems composed of particles. We introduce in the next paragraphs some models describing the microscopic modeling of polymeric liquids.

#### 2.1.4.2 Kinetic Theory Description of Polymeric Liquids.

For the sake of simplicity we focus on polymer solutions (the entangled systems related to the polymer melts can be also described in the kinetic theory framework [17, 18]). We address the Bead-Spring-Chain (BSC) model of polymer solutions. The BSC chain consists of  $S + 1$  beads connected by  $S$  springs. The bead serves as an interaction point with the solvent and the spring contains the local stiffness information depending on local stretching (see [17] for more details). From now on we are also assuming a fully developed homogeneous flow. Thus, the microstructural state does not depend on the space coordinates.

The dynamics of the chain is governed by viscous drag, Brownian and connector forces. If we denote by  $\dot{\mathbf{r}}_k$  the velocity of bead  $k$  and by  $\dot{\mathbf{q}}_k$  the velocity of the spring connector  $\mathbf{q}_k$ , we have

$$\dot{\mathbf{q}}_k = \dot{\mathbf{r}}_{k+1} - \dot{\mathbf{r}}_k \quad \forall k = 1, \dots, S. \quad (2.21)$$

The dynamics of each bead can be written as:

$$\underbrace{-\zeta(\dot{\mathbf{r}}_k - \mathbf{v}_0 - \nabla \mathbf{v} \cdot \mathbf{r}_k)}_{\text{Viscous drag}} - \underbrace{k_b T \frac{\partial \ln(\psi)}{\mathbf{r}_k}}_{\text{Brownian effects}} + \underbrace{\mathbf{F}_k^c - \mathbf{F}_{k-1}^c}_{\text{Connector forces}} = 0, \quad (2.22)$$

where  $\zeta$  is the drag coefficient,  $\mathbf{v}$  is the velocity field,  $\mathbf{v}_0$  is an average velocity,  $k_b$  is the Boltzmann constant,  $T$  is the absolute temperature and  $\psi$  is the distribution function  $\psi(\mathbf{r}_1, \dots, \mathbf{r}_{S+1}, t)$ . From Eqs. (2.21) and (2.22) we obtain:

$$\dot{\mathbf{q}}_k = \nabla \mathbf{v} \cdot \mathbf{q}_k - \frac{1}{\zeta} \sum_{l=1}^S \mathbf{A}_{kl} \cdot \left( k_b T \frac{\partial \ln(\psi)}{\partial \mathbf{q}_l} + \mathbf{F}_l^c \right), \quad (2.23)$$

where  $\mathbf{A}_{kl}$  are the components of the Rouse matrix (see [17] for more details).

In the Rouse model the connector force  $\mathbf{F}^c$  is a linear function of the connector vector, but we could use Finitely Extensible Nonlinear Elastic (FENE) springs, with a dimensionless connector force given by:

$$\mathbf{F}^c(\mathbf{q}_k) = \frac{1}{1 - \mathbf{q}_k^2/b} \mathbf{q}_k, \quad (2.24)$$

where  $\sqrt{b}$  is the maximum dimensionless length of each spring connector of the chain.

Introducing Eq. (2.23) in the equation governing the evolution of the distribution function, and considering homogeneous flows,

$$\frac{\partial \psi(\mathbf{q}_1, \dots, \mathbf{q}_S, t)}{\partial t} = - \sum_{k=1}^S \left( \frac{\partial}{\partial \mathbf{q}_k} (\dot{\mathbf{q}}_k \psi(\mathbf{q}_1, \dots, \mathbf{q}_S, t)) \right), \quad (2.25)$$

we obtain

$$\begin{aligned} \frac{\partial \psi}{\partial t} = & - \sum_{k=1}^S \left( \frac{\partial}{\partial \mathbf{q}_k} \left( (\nabla \mathbf{v} \cdot \mathbf{q}_k - \frac{1}{\zeta} \sum_{l=1}^S \mathbf{A}_{kl} \cdot \mathbf{F}_l^c) \psi \right) \right) \\ & + \frac{k_b T}{\zeta} \sum_{k=1}^S \sum_{l=1}^S \mathbf{A}_{kl} \frac{\partial^2 \psi}{\partial \mathbf{q}_k \partial \mathbf{q}_l}. \end{aligned} \quad (2.26)$$

The micro–macro bridging is performed by computing the virial stress, that within the rheology community is known as Kramer’s rule. The main difficulty in using this description is the highly multidimensional problem defined by Eq. (2.26) that needs specific advanced solvers such as the ones that we proposed in some of our former works within the PGD framework.

### 2.1.4.3 Kinetic Theory Description of Rod-Like Suspensions in Complex Flows

In the case of a dilute suspension of rod-like particles (short fibers, nanofibers, functionalized carbon nanotubes or even rod-like molecules), the configuration distribution function (also known as orientation distribution function) gives the probability of finding the particle in a given direction. Obviously, this function depends on the physical coordinates (space and time) as well as on the configuration coordinates, that taking into account the rigid character of the particles, are defined on the surface of the unit sphere. Thus, we can write  $\psi(\mathbf{x}, t, \mathbf{p})$ , where  $\mathbf{x}$  defines the position of the rod center of mass,  $t$  the time and  $\mathbf{p}$  the unit vector defining the rod orientation. The evolution of the distribution function is given by the Fokker-Planck equation

$$\frac{d\psi}{dt} = -\frac{\partial}{\partial \mathbf{p}}(\psi \dot{\mathbf{p}}) + \frac{\partial}{\partial \mathbf{p}} \left( D_r \frac{\partial \psi}{\partial \mathbf{p}} \right) \quad (2.27)$$

where  $d/dt$  represents the material derivative,  $D_r$  is a diffusion coefficient and  $\dot{\mathbf{p}}$  is the particle rotation velocity. The orientation distribution function must verify the normality condition:

$$\int_{S(0,1)} \psi(\mathbf{p}) d\mathbf{p} = 1 \quad (2.28)$$

where  $S(0, 1)$  denotes the surface of the unit sphere.

For ellipsoidal particles and when the suspension is dilute enough, the rotation velocity can be obtained from the Jeffery's equation

$$\dot{\mathbf{p}} = \boldsymbol{\Omega} \cdot \mathbf{p} + k \mathbf{D} \cdot \mathbf{p} - k(\mathbf{p}^T \cdot \mathbf{D} \cdot \mathbf{p}) \mathbf{p} \quad (2.29)$$

where  $\boldsymbol{\Omega}$  and  $\mathbf{D}$  are the vorticity and the strain rate tensors respectively, associated with the fluid flow undisturbed by the presence of the suspended particles, and  $k$  is a scalar which depends on the particle aspect ratio  $\lambda$  (ratio of its length and diameter)

$$k = \frac{\lambda^2 - 1}{\lambda^2 + 1}, \quad (2.30)$$

that for rod-like particles can be assumed  $k \approx 1$ .

In complex flows simulations the solution of the Fokker-Planck equation involves some numerical difficulties related to: (i) its multidimensional character, i.e.,  $\psi(\mathbf{x}, t, \mathbf{p}) : \Omega \subset \mathbb{R}^3 \times \mathbb{R}^+ \times S(0, 1) \rightarrow \mathbb{R}^+$ ; (ii) the geometrical complexity of the physical domain  $\Omega$ ; (iii) its purely advective character in the physical space; and (iv) the advection effects in the conformation space. Both last behaviors need appropriate numerical stabilizations (e.g. upwinding) of discrete models.

## 2.2 Advanced Solvers for Multi-dimensional Models

The solution of models like the one just addressed in Eq. (2.26) needs new advanced numerical strategies, because the standard ones suffer the curse of dimensionality. Some strategies have been recently proposed for solving models defined in multi-dimensional spaces. The sparse grid techniques are one of the most popular [19], but as we described in the first section, separated representations were also used for solving the models encountered in quantum mechanics (Hartree-Fock and post-Hartree-Fock techniques).

The sparse grids [19] are restricted (as argued in [20]) for treating models involving up to twenty dimensions. On the other hand, separated representations like the one considered in the multi-configuration-self-consistent-fields [2]. We retained the PGD

technology thoroughly described in the previous chapter that allows circumventing efficiently the curse of dimensionality.

## 2.3 Numerical Examples

In this section we illustrate the application of separated representations to the solution of different models defined in highly multidimensional spaces suffering the so-called curse of dimensionality encountered in the finest description of materials.

### 2.3.1 On the Separated Representation of the Schrödinger Equation

Finally we consider a challenging problem, the one associated with the solution of the Schrödinger equation introduced in Sect. 2.1.1.

In this case to circumvent the curse of dimensionality that this model involves we could try to perform, as in the previous examples, a separated representation of the wavefunction  $\Psi$ .

In what follows we consider a system composed of  $N$  electrons and a single nucleus with atomic number  $Z = N$ . In this case one could assume the time-independent wavefunction approximation:

$$\Psi(\mathbf{x}_1, \dots, \mathbf{x}_N; \mathbf{X}) \approx \sum_{j=1}^{j=n} \alpha_j \phi_j^1(\mathbf{x}_1) \cdot \phi_j^2(\mathbf{x}_2) \cdot \dots \cdot \phi_j^N(\mathbf{x}_N) \quad (2.31)$$

where  $\mathbf{X}$  denotes the nucleus position.

However, the Pauli's exclusion principle that applies for fermions (electrons belong to the fermions family) implies the antisymmetry of the wavefunction. To ensure the antisymmetry one could proceed by introducing the Slater's determinants:

$$D_j = \begin{vmatrix} \phi_j^1(\mathbf{x}_1) & \phi_j^2(\mathbf{x}_1) & \dots & \phi_j^N(\mathbf{x}_1) \\ \phi_j^1(\mathbf{x}_2) & \phi_j^2(\mathbf{x}_2) & \dots & \phi_j^N(\mathbf{x}_2) \\ \vdots & \vdots & \ddots & \vdots \\ \phi_j^1(\mathbf{x}_N) & \phi_j^2(\mathbf{x}_N) & \dots & \phi_j^N(\mathbf{x}_N) \end{vmatrix} \quad (2.32)$$

that, introduced in the separated representation

$$\Psi(\mathbf{x}_1, \dots, \mathbf{x}_N; \mathbf{X}) \approx \sum_{j=1}^{j=n} \alpha_j D_j \quad (2.33)$$

ensures the antisymmetry of the resulting wavefunction.



However, the last representation hides two difficulties. The first one is related to the multidimensional character of the model (we must recall that the wavefunction is defined in a space of dimension  $3 \times N$ ) and the second one is related to the complexity in evaluating the Slater determinants that scales in  $N!$ . In order to isolate each difficulty, we are considering an “imaginary world” in which the electrons are not subjected to the Pauli’s exclusion principle. In this case the separated representation (2.31) works and it could be used to solve the Schrödinger equation.

For the sake of simplicity, in what follows, we assume that each electron “lives” in a 1D dimensional space, i.e.,  $\Psi(x_1, \dots, x_N; X)$ , where  $x_k \in \mathbb{R}$ ,  $\forall k$ .

Now, we consider different systems containing the more and more electrons:  $N = 1, 2, 3, 4, 5, 10, 20, 50$ . In the last case the Schrödinger equation is defined in a space of dimension 50.

For each system, the time independent Schrödinger equation (2.4) is solved using the separated representation (2.31), and the ground state eigenvalue  $\Psi_0$  and its associated energy  $E_0$  is computed. Now, the ground state electronic distribution  $\rho^0(x)$  can be obtained by calculating the ground state distribution of each electron  $e$ ,  $\rho_e^0$ :

$$\rho_e^0(x) = \int_{\mathbb{R}^{N-1}} |\Psi_0(x_1, \dots, x_{e-1}, x_{e+1}, \dots, x_N)|^2 dx_1 \dots dx_{e-1} dx_{e+1} \dots dx_N \quad (2.34)$$

and adding all the electrons’ contributions

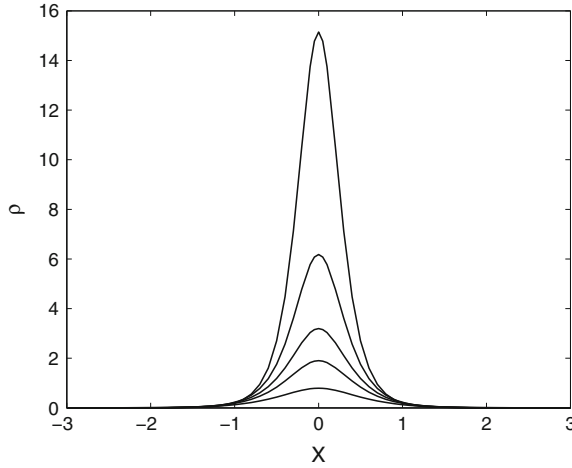
$$\rho^0(x) = \sum_{e=1}^{e=N} \rho_e^0. \quad (2.35)$$

Figure 2.1 depicts the ground-state electronic distribution for  $N = 1$ ,  $N = 2$ ,  $N = 3$ ,  $N = 5$  and  $N = 10$ . Obviously the electronic distribution is concentrated around the nucleus position and increases as the number of electrons increases. In that figure, to ensure a good quality in the curves resolution we do not include the electronic distributions of the systems composed of 20 and 50 electrons.

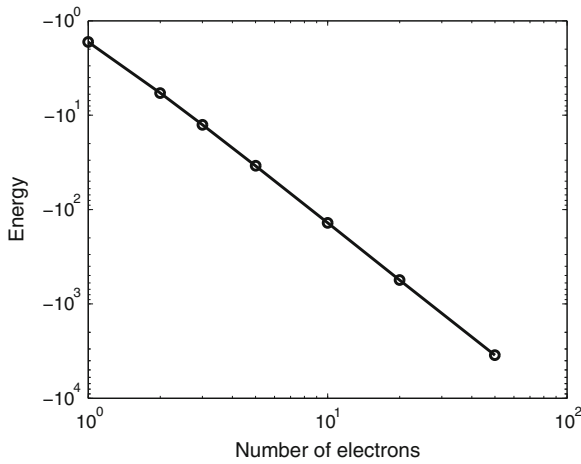
It is easy to verify that because the Pauli’s exclusion principle does not apply,  $\rho^0(N) = N\rho^0(1)$ , where  $\rho^0(N)$  and  $\rho^0(1)$  denote the ground state densities of systems composed of  $N$  and 1 electrons respectively. Thus, we can conclude that all the electrons are occupying the same orbital, a kind of  $s$ -orbital (that in 3D systems would be spherical).

Figure 2.2 depicts for these “imaginary” systems the evolution of the ground state energy (the most negative eigenvalue related to the solution of Eq. (2.4)) as a function of the number of electrons involved in the system.

From this analysis we conclude that separated representation allows us to circumvent the curse of dimensionality related to quantum mechanics systems, making possible the treatment of multidimensional models. However, the previous analysis concerns “non-real” systems, because electrons are fermions, and for fermions the Pauli’s principle applies.



**Fig. 2.1** Ground state electronic density for systems composed of 1, 2, 3, 5 and 10 electrons—the Pauli’s principle has not been applied



**Fig. 2.2** Evolution of the ground state energies with the number of electrons involved in the system—the Pauli’s principle has not been applied

Even if separated representations could be applied for solving bosonic quantum systems (the Pauli’s principle does not apply for bosons) in material science such systems have a limited interest. For this reason we must come back to the “real world” of electronic systems.

In the present case, the separated representation to be considered is the one making use of the Slater determinants (2.33). All the practical details concerning the discretization of the Schrödinger equation by using a wavefunction separated representation within the Slater’s determinants formalism can be found in [21]. In this

case, as the complexity scales with the factorial of the number of electrons involved in the quantum system, at present, in our knowledge, only small systems can be solved (containing up to ten electrons).

Figure 2.3 depicts the ground state electronic distribution of systems composed of 1 to 5 electrons and a single nucleus with atomic number  $Z = 3$ . It also shows the differences between each two successive configurations. We can notice that the first two electrons are located in an  $s$ -type orbital (both electrons have different spin which makes it possible). For more than two electrons we appreciate the appearance of  $p$ -type orbitals. These  $p$ -type orbitals can be identified by subtracting the electronic density functions related to both kind of populations (up to two electrons and more than two electrons).

Figure 2.4 compares the evolution of the ground state energy with the number of electrons  $N$  involved in the quantum system composed on a single nucleus with  $Z = N$ , when the Pauli's principle is or is not taken into account. For comparison purposes, when the Pauli's exclusion principle was activated, the spin coordinate was removed, because in this way each electron is forced to occupy a different orbital (as was the case when the Pauli's principle was not taken into account). We can notice that its consideration increases the value of the ground state energy.

From the previous analysis we can affirm that the remaining unsolved difficulty related to the solution of the Schrödinger equation lies in the antisymmetry restriction that the Pauli's principle addresses for fermions, and that as previously argued, its complexity scales as  $N!$ , which becomes extremely large even for systems composed of a moderate number of electrons.

### 2.3.2 Kinetic Theory Description of Rod-Like Aggregating Suspensions

In this section we come back to the suspension model summarized in Sect. 2.1.4. In order to increase the model complexity we are assuming that the rods can flocculate creating large aggregates that due to the shear induced by the flow, are continuously broken. Thus, aggregation and disaggregation mechanisms coexist and two populations can be identified: the one related to free rods (pendant population) and the one associated with the aggregated rods (active population). Figure 2.5 depicts both populations and the flow induced aggregation/disaggregation.

The kinetic theory description of such systems contains two coupled Fokker-Planck equations given the orientation distribution of rods belonging to each one of these populations,  $\Psi(\mathbf{x}, t, \mathbf{p})$  and  $\Phi(\mathbf{x}, t, \mathbf{p})$  for the active and pendant respectively:

$$\frac{d\Psi}{dt} = -\frac{\partial}{\partial \mathbf{p}}(\dot{\mathbf{p}}\Psi) + D_{r1}\frac{\partial^2 \Psi}{\partial \mathbf{p}^2} - V_d\Psi + V_c\Phi, \quad (2.36)$$

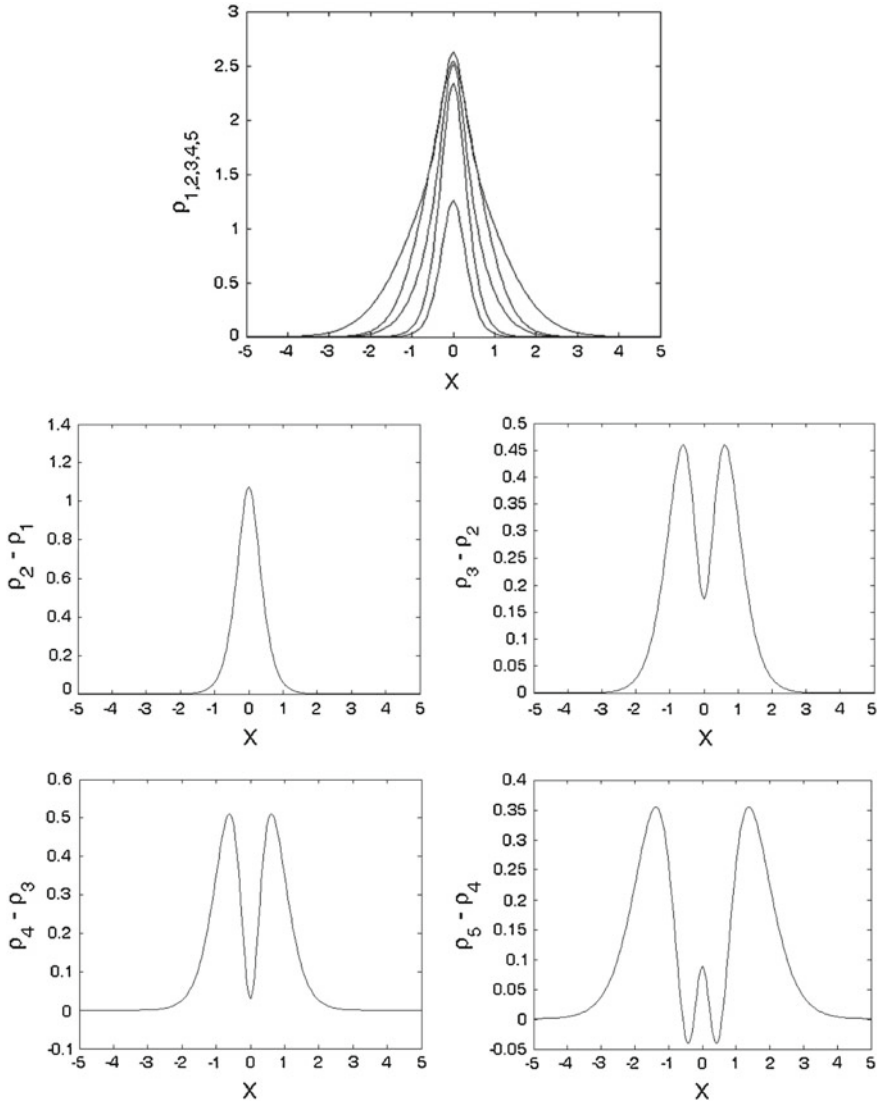


**Fig. 2.3** Ground state electronic density for systems composed of 1, 2, 3, 4 and 5 electrons—Pauli principle applies

$$\frac{d\Phi}{dt} = -\frac{\partial}{\partial \mathbf{p}} (\dot{\mathbf{p}}\Phi) + D_{r2} \frac{\partial^2 \Phi}{\partial \mathbf{p}^2} + V_d \Psi - V_c \Phi, \quad (2.37)$$

where  $V_d$  and  $V_c$  represent the velocity of destruction and construction of the active population respectively.

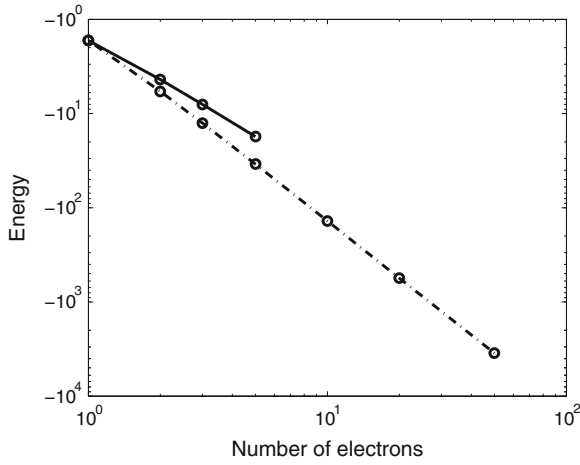


**Fig. 2.4** Evolution of the ground state energy when the Pauli's principle is activated

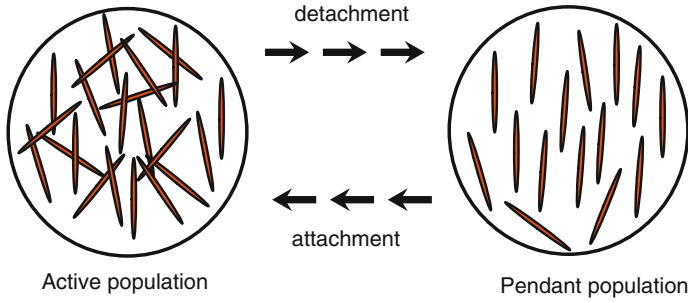


**Fig. 2.5** Flow induced aggregation/disaggregation

The normality condition is written

$$\int_{S(0,1)} (\Psi(\mathbf{x}, t, \mathbf{p}) + \Phi(\mathbf{x}, t, \mathbf{p})) d\mathbf{p} = 1, \quad \forall \mathbf{x}, \forall t. \quad (2.38)$$

We consider that the flow takes place in a converging channel. The steady state flow kinematics (assumed undisturbed by the presence of the suspended particles) was computed by solving the Stokes equations.

As we are interested in computing the steady state solution, and because the advection character of the Fokker-Planck equations in the spatial coordinates ( $\mathbf{x}$ ), we decided to integrate both coupled Fokker-Planck equations along some particular flow streamlines. The separated representation of both orientation distribution functions writes:

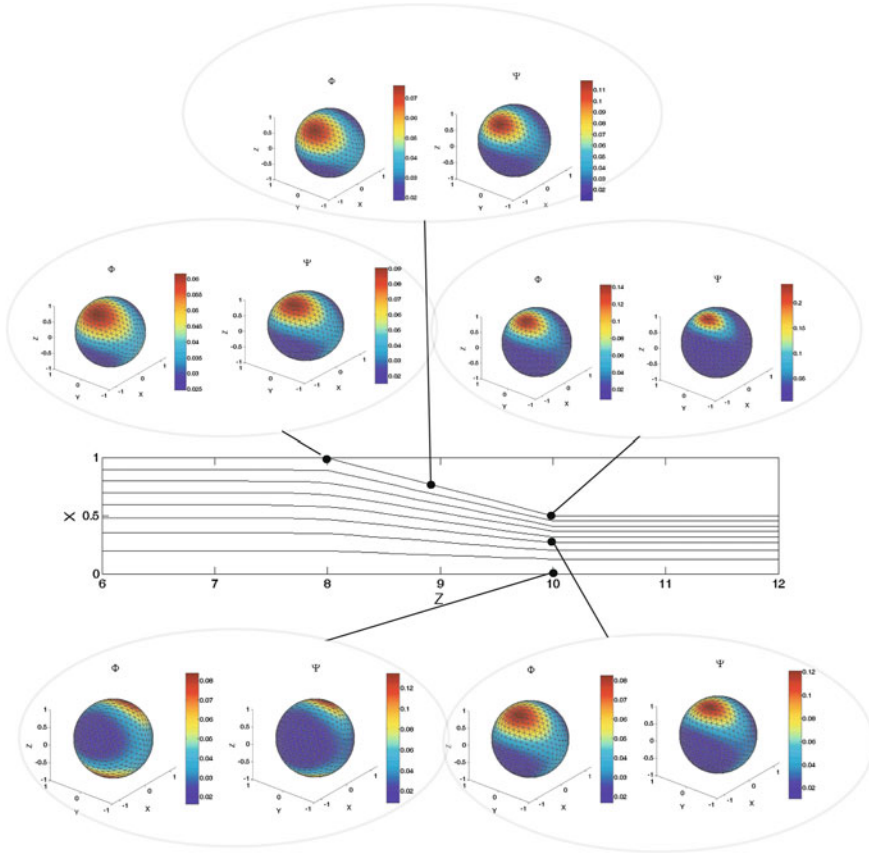


**Fig. 2.6** Orientation distribution of active and pendant populations in a contraction flow

$$\begin{pmatrix} \Psi_{st}(s, \mathbf{p}) \\ \Phi_{st}(s, \mathbf{p}) \end{pmatrix} = \sum_{j=1}^n \begin{pmatrix} \alpha_j^{st} E_j^{st}(\mathbf{p}) F_j^{st}(s) \\ \beta_j^{st} G_j^{st}(\mathbf{p}) H_j^{st}(s) \end{pmatrix} \quad (2.39)$$

where  $s$  denotes the curvilinear coordinate defining the streamlines, and the index “ $st$ ” refers to the particular streamline along which the integration is performed.

Figure 2.6 depicts the resulting orientation distributions of both populations at some points on some flow streamlines. In this figure the orientation distribution is directly depicted on the unit surface, and the colors indicate the intensity of the orientation in each direction.

## 2.4 Conclusions

In this chapter we revisited different physical descriptions at different scales involved in material science. At the lowest scale, quantum mechanics involves high-dimensional models whose solution, when fermions are considered, must be anti-symmetric. We have pointed out that in fact, more than the multidimensional character of quantum mechanics models, the real challenge is the antisymmetry constraint.

Coarser modeling involves molecular dynamics or Brownian dynamics but despite its conceptual simplicity its use is not exempted from computational and conceptual difficulties. The next level is the one that corresponds to statistical mechanics descriptions leading to continuous models described by non-linear and coupled multidimensional partial differential equations. Some of these models have been successfully solved in some of our former works by using the adaptive separated representation within the PGD framework. This technique seems a promising alternative for addressing highly-multidimensional models, but as argued in the previous section, its use in quantum mechanics systems composed of fermions is limited, at present, by the antisymmetry restriction.

## References

1. E. Cancès, M. Defranceschi, W. Kutzelnigg, C. Le Bris, Y. Maday, in *Computational Quantum Chemistry: a Primer*. Handbook of Numerical Analysis, vol 10 (Elsevier, Amsterdam, 2003), p. 3–270
2. C. Le Bris (ed.), *Handbook of Numerical Analysis*. Computational Chemistry, Vol. 10 (Elsevier, Amsterdam, 2003)
3. V. Gavini, K. Bhattacharya, M. Ortiz, Quasi-continuum orbital-free density-functional theory: a route to multi-million atom non-periodic DFT calculation. *J. Mech. Phys. Solids* **55**(4), 697–718 (2007)
4. C. Le Bris, P.L. Lions, From atoms to crystals: a mathematical journey. *Bull. Am. Math. Soc.* **42**(3), 291–363 (2005)
5. C. Le Bris, Computational chemistry from the perspective of numerical analysis. *Acta Numerica* **14**, 363–444 (2005)
6. C. Le Bris, in *Mathematical and Numerical Analysis for Molecular Simulation: Accomplishments and Challenges*. Proceedings of the International Congress of Mathematicians, (Madrid, Spain, 2003), pp. 1507–1522
7. V.B. Shenoy, R. Millera, E.B. Tadmor, D. Rodney, R. Phillips, M. Ortiz, An adaptive finite element approach to atomic-scale mechanics—the quasicontinuum method. *J. Mech. Phys. Solids* **36**, 500–531 (1999)
8. G.J. Wagner, W.K. Liu, Coupling of atomistic and continuum simulations using a bridging scale decomposition. *J. Comput. Phys.* **190**, 249–274 (2003)
9. H. Ben Dhia, Multiscale mechanical problems: the Arlequin method. *C. R. Acad. Sci., Paris* 326, Ser-II b. **326**, 899–904 (1998)
10. S.P. Xiao, T. Belytschko, A bridging domain method for coupling continua with molecular dynamics. *Comput. Methods Appl. Mech. Eng.* **193**, 1645–1669 (2004)
11. H.C. Öttinger, M. Laso, in *Smart Polymers in Finite Element Calculation*, ed. by P. Moldanaers, R. Keunings. Theoretical and Applied Rheology. Proceedings of the XIth International Congress on Rheology, vol 1 (Elsevier, 1992), pp. 286–288

12. M.A. Martinez, E. Cueto, I. Alfaro, M. Doblare, F. Chinesta, Updated Lagrangian free surface flow simulations with the natural neighbour Galerkin methods. *Int. J. Numer. Meth. Eng.* **60**(13), 2105–2129 (2004)
13. D. Gonzalez, E. Cueto, F. Chinesta, M. Doblare, An updated Lagrangian strategy for free-surface fluid dynamics. *J. Comput. Phys.* **223**, 127–150 (2007)
14. M.A. Martinez, E. Cueto, M. Doblare, F. Chinesta, Natural element meshless simulation of injection processes involving short fiber suspensions. *J. Nonnewton. Fluid Mech.* **115**, 51–78 (2003)
15. A. Ammar, B. Mokdad, F. Chinesta, R. Keunings, A new family of solvers for some classes of multidimensional partial differential equations encountered in kinetic theory modeling of complex fluids. *J. Nonnewton. Fluid Mech.* **139**, 153–176 (2006)
16. F. Chinesta, A. Ammar, A. Falco, M. Laso, On the reduction of stochastic kinetic theory models of complex fluids. *Model. Simul. Mater. Sci. Eng.* **15**, 639–652 (2007)
17. B.B. Bird, C.F. Curtiss, R.C. Armstrong, O. Hassager, in *Dynamics of Polymeric Liquids. Kinetic Theory*, vol 2 (John Wiley and Sons, Chichester, 1987)
18. R.G. Larson, *The Structure and Rheology of Complex Fluids* (Oxford University Press, New York, 1999)
19. H.J. Bungartz, M. Griebel, Sparse grids. *Acta Numerica* **13**, 1–123 (2004)
20. Y. Achdou, O. Pironneau, *Computational Methods for Option Pricing*, *SIAM Frontiers in Applied Mathematics* (SIAM Publishers, Philadelphia, 2005)
21. A. Ammar, F. Chinesta, in *Circumventing Curse of Dimensionality in the Solution of Highly Multidimensional Models Encountered in Quantum Mechanics Using Meshfree Separated Representations*. *Lecture Notes on Computational Science and Engineering*, (Springer, 2008), pp. 1–17



PGD-Based Modeling of Materials, Structures and  
Processes

Chinesta, F.; Cueto, E.

2014, XVII, 219 p. 84 illus., Hardcover

ISBN: 978-3-319-06181-8